Original Paper

Influence of structural boron on 'illite crystallinity': results from mud volcanoes in Azerbaijan

Matteo Salvadori[1,2] , Stefano Battaglia[1], Marco Lezzerini[2] , Dadash Huseynov[3] and Maddalena Pennisi[1]

[1]Istituto di Geoscienze e Georisorse, Via Moruzzi 1, 56124 Pisa, Italy; [2]Dipartimento di Scienze della Terra, Via Santa Maria 53, 56126 Pisa, Italy and [3]Institute of Geology and Geophysics, Azerbaijan National Academy of Sciences, Azerbaijan

Abstract

Sedimentary volcanism is a widespread phenomenon on Earth that leads to the extrusion of fine-grained sediments, saline waters, and hydrocarbons in compressional environments. In the present study, mud volcanoes located in eastern Azerbaijan were investigated with a particular interest in boron (B) influence on illite crystallinity, compared with results reported in the literature for Northern Apennine mud volcanoes (Italy). Azerbaijan sediments have a predominant silt fraction and a mineralogy dominated by quartz, feldspar, calcite, and clay minerals (illite, mixed-layer illite smectite, smectite, and chlorite). Reichweite grade, measured by estimated illite percentage in Ilt-Sme, associated with a geothermal gradient of 18°C km^{-1}, indicates a sediment origin of 7–8 km, consistent with the depth of the Maikop Series, considered in the literature to be the main source rock of the erupted muds. Azerbaijan samples confirmed the inverse correlation between structural B in illite (53–182 μg g^{-1}) and the Kübler index (KI) on illite (0.53–0.71°Δ2θ), previously observed for mud volcanoes in the Apennines. This suggests that a common process operates in these different environments, highlighting the role of B in illite crystallinity, and confirming the need to consider this interaction when using KI as a sediment depth marker in similar geological contexts.

Keyword: Apennine mud volcanoes; Azerbaijan mud volcanoes; boron; clay minerals; formation waters; illite crystallinity

Introduction

Mud volcanoes, also referred to as sedimentary volcanoes, form in regions where layers of fluidized sediments, such as silt and clay, undergo pressurization due to tectonic activity, such as in convergent plate boundary zones or through accumulation of hydrocarbon gases (Brown, 1990; Bonini, 2012). At the surface, mud volcanoes release pressurized gas, of which >90% by volume is methane, with a lesser amount of carbon dioxide and nitrogen (Kopf, 2003), and saline water, occasionally enriched with traces of oil. These geological phenomena offer invaluable insights into the intricate processes governing the formation and migration of oil and gas, reaching depths up to 11 km (Mazzini and Etiope, 2017). The erupted water is rich in organic compounds, as well as in Br, B, Cl, I, and, eventually, Li (Mazzini and Etiope, 2017; Nikitenko and Ershov, 2021). Volcanic edifices, reaching a height of a few hundred meters, can sprawl over several square kilometers. Notably, Azerbaijan (AZ) and the Caspian Sea have the highest concentration of mud volcanoes worldwide and are home to some of the largest of them (Mazzini and Etiope, 2017; Baloglanov et al., 2018).

Boron is generally enriched in clay minerals and saline water associated with sedimentary volcanism (Kopf and Deyhle, 2002). Based on quantitative clay mineralogy and the boron (B) content in mud, studies showed that with the advancing of smectite illitization in the B-rich fluid environment, fluid–mud interaction induces B to enter into the illite structure (Frederickson and Reynolds, 1960; Williams et al., 2001a).

In their study of mud products from Northern Apennines (NA) mud volcanoes, Battaglia and Pennisi (2016), suggested that B-rich water associated with mud volcanism can affect 'illite crystallinity', and support that hydro-chemical environment exerts an influence on the intensity of post-sedimentary transformations (Buryakovsky et al., 1995). The principal clay mineral sorbent is illite; however, other clay minerals such as smectite, chlorite, kaolinite, and mixed-layer illite-smectite can also contain significant amounts of B (Frederickson and Reynolds, 1960; Palmer et al., 1987; Ishikawa and Nakamura, 1993; Williams et al., 2001a).

Illite formed in a B-rich environment adsorbs B rapidly on its surface and B then diffuses slowly into the tetrahedral part of the structure where it replaces Si and/or Al (Fig. 1; Goldberg and Arrhenius, 1958; Couch and Grim, 1968; Stubican and Roy, 1962; Fleet, 1965; Keren and O'Connor, 1982; Williams and Hervig, 2002; Williams et al., 2001a; Williams et al., 2001b). Direct evidence of the substitution of B into the tetrahedral sheet of the structure was obtained using infrared spectroscopy by Stubican and Roy (1962).
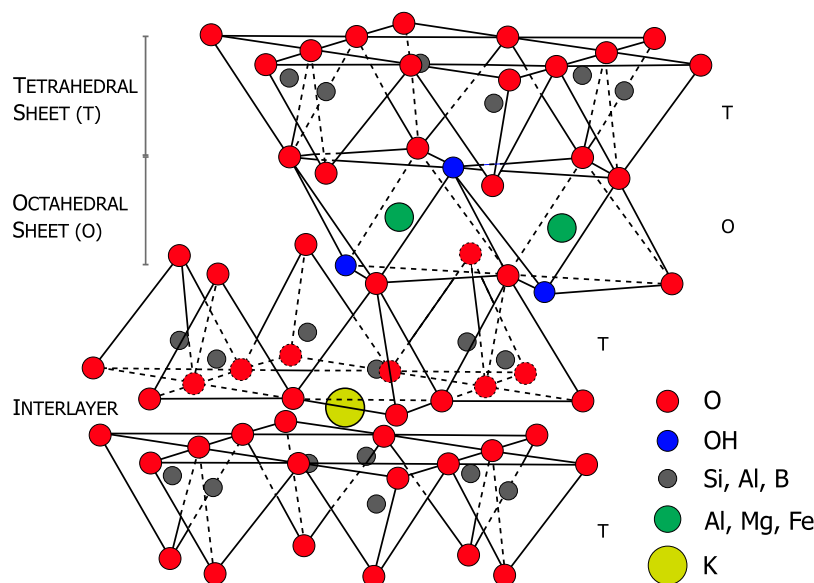
Figure 1. Schematic representation of the illite structure (modified from Murray, 2006).

Molecular modeling of the illite structure using density functional theory revealed that B incorporation is energetically favored in tetrahedral sites, replacing Si atoms, rather than in the interlayer of expandable clays (Williams et al., 2007; Clauer et al., 2018; Martos-Villa et al., 2020). Given that the B tetrahedral covalent radius is smaller (B: 88 pm; Al: 126 pm; Si: 117 pm; Shannon, 1976; Bailey, 2006), boron replacement of Si and/or Al in tetrahedral sites has the effect of changing the illite cell dimension, and the degree of 'illite crystallinity,' expressed in general as the Kübler index (KI), established as the full width at half-maximum height value (FWHM) of the (001) illite peak (Kübler, 1964; Kübler, 1967; Kübler, 1984).

The understanding gained on Northern Apennine mud volcanoes was expected to influence the KI in the sedimentary sequence at the illite–smectite transition. The conversion of smectite into illite depends on numerous factors such as availability of K^+ in the system, reaction time, chemistry of the circulating fluids, and to a large extent on temperature and pressure (Colten-Bradley, 1987). Moreover, modification in smectite ordering and a progressive reduction in smectite content within mixed-layer illite-smectite (Ilt-Sme) occurring during burial have been utilized as mineral markers to define the thermal history of sedimentary sequences and trace diagenetic and low-grade metamorphic reactions (Velde et al., 1986; Velde and Vasseur, 1992; Pollastro, 1993; Hillier et al., 1995; Varajao and Meunier, 1996; Lanson et al., 1998; Berger et al., 1999). In this setting, Ilt-Sme clay minerals are commonly utilized as a mineral thermal indicator; as physical and chemical conditions change during burial, smectites become unstable and are converted to illite via transitional mixed-layer Ilt-Sme (abbreviations after Warr, 2021).

In the present study, previous investigations on the effect of boron on 'illite crystallinity' (Battaglia and Pennisi, 2016) were extended to three mud volcanoes in Eastern Azerbaijan (Perikushkul, Dashgil, and Shikhzahirli), and a comparison between the two case studies is discussed. The main objective is to explore the relationship between structurally fixed boron in illite and the KI, investigated here from a mineralogical and geochemical perspective. New insights are provided into the clay mineral phases,

boron (and potassium) contents in the clay fraction (<2 μm), and physical properties, such as sediment grain size, of the AZ mud volcanoes, contributing data that are currently scarce in the literature.

Geological framework

Since the Plio-Pleistocene age, most of the convergence in the Eastern Caucasus region has been accommodated by the Kura Fold-and-Thrust Belt (FTB), located in the southeastern section of the Greater Caucasus. This domain has highly variable characteristics with isolated thrust folds propagating out of sequence in the western part and duplex structures with sequenced thrusts in the eastern part. The structures, which deform the Plio-Quaternary sedimentary deposits of the Kura basin, have a southward trend with shallow detachments (~5 km), located in the clayey formation of Maykop (Oligocene-Miocene) (Allen et al., 2003). Mud volcanoes in Azerbaijan are sited in the FTB area, mainly in the eastern part, and offshore in the South Caspian Basin (SCB). They generally develop on the crests of anticlinal folds that deform the fluvio-deltaic deposits of the Kura basin (up to 6 km thick and aged between the Upper Miocene and Lower Pliocene), and, generally, form edifices that have an elliptical base with a major axis parallel to the direction of maximum local horizontal stress (Bonini, 2012). The Kura is a foreland sedimentary basin of the Great Caucasus, consisting of a very thick synorogenic sedimentary sequence (up to 10 km onshore and 25 km in the SCB) of Paleocene-Quaternary age (Bonini et al., 2013). In the Oligocene-Lower Miocene rapid deposition of an anoxic level of fine sediments, rich in organic matter, with a variable thickness between 200 and 1200 m and continuous throughout the region, is recorded in the basin, which is known as the Maykop (Hudson et al., 2008). This formation, the top of which is attested at a depth between 4 and 6 km in eastern Azerbaijan and reaches the surface in the Great Caucasus area, represents the detachment level of the FTB and the primary source of hydrocarbons and sediments that generate mud volcanoes (Kopf et al., 2003). Above the Maykop

Series is placed the formation of the Diatom Suite (Middle-Upper Miocene), which presents shale and marl with interlayers of sandstone and pelite. In the Lower Pliocene-Upper Miocene the sedimentation rate underwent a notable increase with the deposition of the Productive Series, formed by fluvio-deltaic deposits with interlayers of shale. This formation reaches a thickness of 5–7 km in the central part of the SCB and hosts the hydrocarbon and mud reservoirs and it is sealed at the top by the marine shales of the Akchagyl Series (Upper Pliocene). The sequence is completed by Quaternary deposits of the non-marine environment of the Absheron Series and recent sediments (Bonini et al., 2013). As a result of the compressive tectonics and the complex system of folds and thrusts, the depth of the Maykop Series (and consequently those above) varies locally within the FTB from 10 to 4 km. Furthermore, although the Maykop Series is inferred as the primary source of mud, clasts belonging to the less recent formations have also been found in the eruptive products, suggesting a mobilization of the material even from deeper reservoirs.

Sampling and experimental methods

Nine mud samples and associated waters extruded from the volcanoes Perikushkul, Dashgil, and Shikhzahirli, located in the Absheron region and from Daghlig–Shirvan in Gobustan (Azerbaijan) (Fig. 2), were collected in July 2017. Five samples were taken from different gryphons at Perikushkul (labeled as P1, P2, P3, P4, P5), where mud was gently pouring out at the time of sampling. Three samples were collected from gryphons at Dashgil (labeled G1, G2, G3), and one sample was taken from the lake at the top of Shikhzahirli volcano (labeled SH), where intense gas bubbling was observed (Fig. 3). Temperature (°C) and electrical conductivity (EC; mS cm^{-1}) were measured during sampling

(Table 1). EC measurements were repeated after one day, once sediment had settled by gravity. Significant separation of the two phases was not observed after 1 day in samples P1, P2, G1, and SH.

The mud samples were stored in plastic bottles. In the laboratory, water was separated from sediments by decantation, after the suspension had settled. Sediments were subsequently dried at $T<60°C$ to avoid any changes in the structure of the clay minerals (Moore and Reynolds, 1997). The dried sludge was gently disaggregated and divided into quarters (Cavalcante and Belviso, 2005) for particle size and mineralogical and chemical analysis. Separated water was filtered using 0.2 μm Sartorius filters, and analyzed for B using inductively coupled plasma-optical emission spectroscopy (Perkin Elmer Optima 2000DV instrument).

Grain size

The grain size of bulk samples was determined using a diffraction pattern analyzer (Malvern Mastersizer 2000, coupled to a Hydro 2000G wet sample dispersion unit: range of measurements 0.1 μm to 2 mm). Replicate analyses yielded 2SD = ±3% (*n*=5).

X-ray powder diffraction

The main mineral phases were identified through X-ray diffraction (XRD) analysis of powdered bulk-rock samples. For XRD analyses of oriented slides, the clay fraction (<2 μm grain size) was separated from the aqueous suspensions of whole-rock powders by differential settling, in accordance with Stokes' law. The aqueous suspension of each fraction was pipetted, saturated with K$^+$ and Mg^{2+} (KCl 1 M and MgCl$_2$ 0.1 M solutions), allowed to settle on the slides, and then dried at room temperature to produce highly oriented preparations. Care was taken to avoid excessively thin preparations; the amount of clay on each slide was within the range of 3–4 mg cm^{-2} (Lezzerini et al., 1995). No specific procedure was applied to remove the organic

Figure 2. Sampled mud volcano sites (in red).

Figure 3. Sampling of muds from active gryphons and mud pools at the Perikushkul and Shikhzahirli mud volcanoes.

Table 1. Sample sites and field data

Site	ID	*T* (°C)	EC (mS cm⁻¹)	EC 24 h
Perikushkul	P1	22.2	19.1	n.d.*
Latitude: 40°28′50.05″N	P2	23.0	17.2	n.d.*
Longitude: 49°26′54.19″E	P3	22.0	14.3	15.7
	P4	23.0	14.2	15.6
	P5	22.0	22.1	22.9
Dashgil	G1	n.d.	21.9	n.d.*
Latitude: 39°59′45.77″N	G2	24.2	24.0	28.7
Longitude: 49°24′11.50″E	G3	19.5	37.5	42.1
Shikhzahirli	SH	n.d.	22.8	n.d.*
Latitude: 40°29′13.39″N				
Longitude: 49°2′6.35″E				

EC = electrical conductivity; n.d. = not determined; n.d.* = not determined, still turbid solution after 24 h.

Figure 4. XRD spectra of bulk-sample powders. Qtz = quartz; Phyll = phyllosilicates; Kfs = K-feldspar; Pl = plagioclase; Cal = calcite. Wavelength = 0.15418 nm.

matter or carbonates to avoid deleterious effects on the phyllosilicates. A 1.82% mannitol solution was used to remove adsorbed B (Williams and Hervig, 2002). The main constituents of mud samples were identified as quartz, feldspars, and calcite, with associated dolomite in some samples (P1, P2, P4, P5, SH) (Fig. 4). Oriented slides indicated the occurrence of smectite, mixed-layer Ilt-Sme, illite, and chlorite (Fig. 5a–c). KI values are reported in Table 2, along with a quantitative analysis of clay-mineral phases in wt.% carried out according to the methodology described by Moore and Reynolds (1997). Instrumental setting and data processing methods were described by Battaglia and Pennisi (2016).
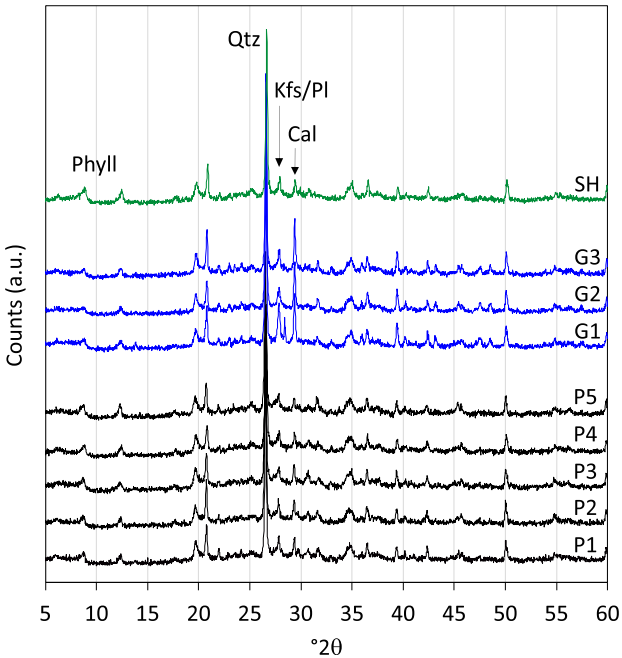
The KI measurements were conducted on ethylene-glycol (EG) oriented slides on the 5 Å peak of the Ilt phase (002 basal peak) to avoid interference with the mixed-layer Ilt-Sme (Battaglia et al., 2004), and were refined with an accurate fitting, as described by Battaglia and Pennisi (2016). To assess the reproducibility and
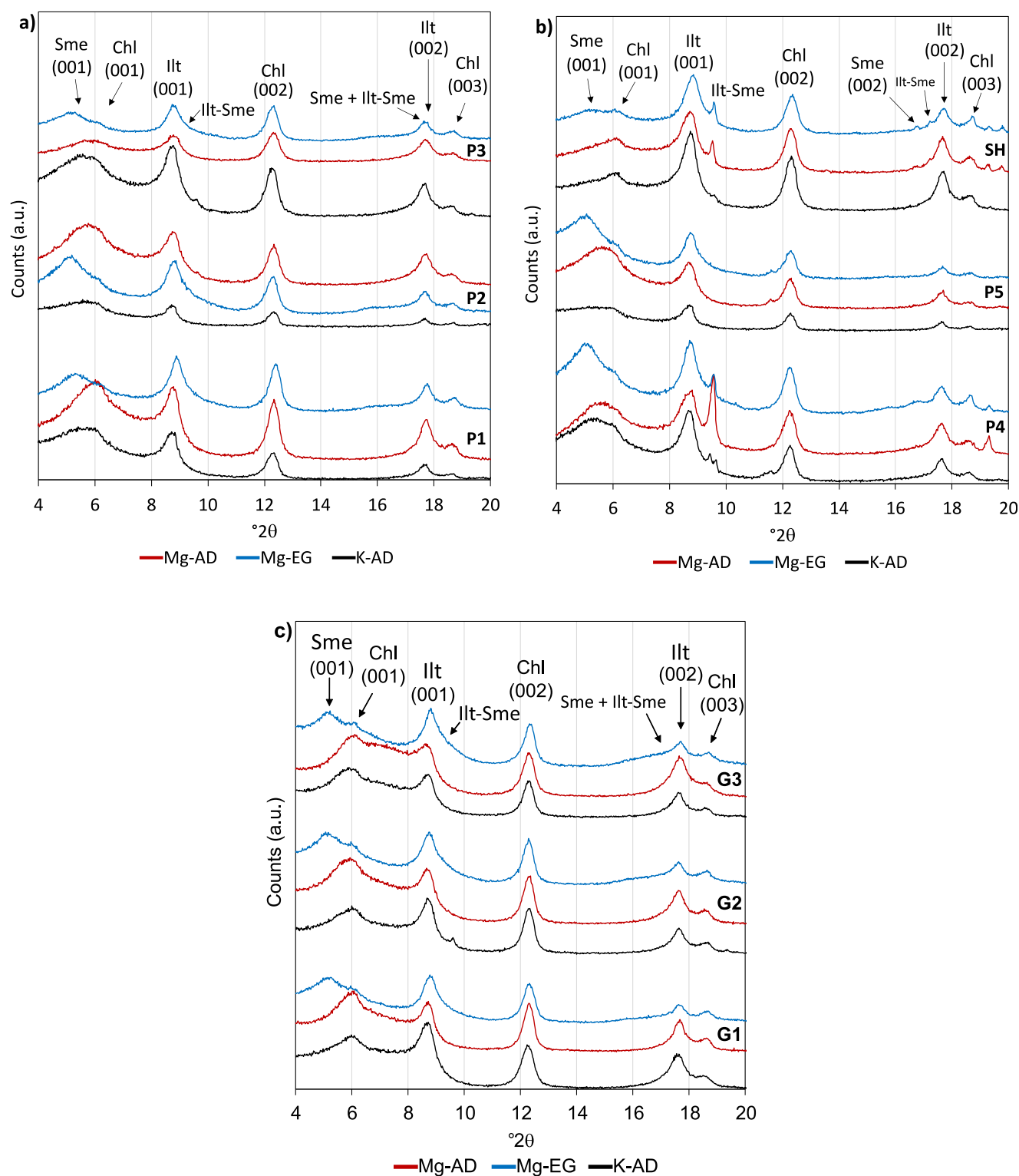
Figure 5. (a–c) XRD spectra of oriented slides from the clay fraction. Sme = smectite; Ilt-Sme = mixed-layer illite-smectite; Ilt = illite; Chl = chlorite; K-AD = samples saturated with KCl solution and air dried; Mg-AD = samples saturated with MgCl$_2$ solution and air dried; Mg-EG = samples saturated with MgCl$_2$ solution and ethylene glycol; wavelength = 0.15418 nm.

accuracy of the results, multiple slides from a single batch of the sample suspension were measured several times. The relative standard deviation of KI measurements was 3–5% for samples with illite-chlorite clay mineral assemblages and 5–8% for those mixed-layer Ilt-Sme. The KI data were calibrated using the standard rock slab series established by Kübler, adhering to the procedures and calibration equation outlined by Leoni (2001).

Quantitatively, the primary diagenetic clay reaction in shale is the gradual conversion of smectite into illite through the formation of mixed-layer Ilt-Sme, a process known as smectite illitization. Reynolds and Hower (1970) were the first to provide a detailed account of the relationship between Ilt-Sme and depth, identifying three interstratification forms of Ilt-Sme characterized by a different 'Reichweite' (R) order (Reynolds, 1980): random (R=0),

Table 2. Mineralogy of clay minerals and associated KI

ID	Sme	Ilt-Sme	Ilt	Chl	KIn
P1	4.4	36.2	49.6	9.9	0.57
P2	7.5	34.2	51.0	7.3	0.63
P3	9.0	28.1	54.3	8.7	0.58
P4	4.9	43.9	43.9	7.3	0.65
P5	7.5	34.3	50.6	7.6	0.53
G1	5.7	23.9	56.9	13.5	0.61
G2	6.6	43.1	38.9	11.4	0.61
G3	4.5	52.2	35.1	8.2	0.71
SH	4.1	18.7	60.3	16.9	0.54

Phases are reported as wt.% of total <2 μm fraction (Sme = smectite; Ilt-Sme = illite-smectite mixed layers; Ilt = illite; Chl = chlorite; mineral abbreviation nomenclature according to Warr, 2021).

Table 3. Reichweite order obtained according to the Moore and Reynolds (1997) calculation method

ID	Percentage illite in Ilt-Sme	R order
P1	62	1
P2	71	1
P3	68	1
P4	68	1
P5	58	0
G1	76	1
G2	74	1
G3	71	1
SH	71	1

Table 4. Structural B concentration of total clay and Ilt are reported in mg kg^{-1}; the Ilt fraction and K_2O content are reported in wt.%

ID	B_{fix} clay	Ilt	B_{fix} Ilt	K_2O
P1	317	49.6	157	3.12
P2	247	51.0	126	3.09
P3	276	54.3	150	2.31
P4	240	43.9	105	2.35
P5	360	50.6	182	2.32
G1	164	56.9	93	2.98
G2	172	38.9	67	2.79
G3	152	35.1	53	3.07
SH	294	60.3	177	3.19

short-range (R=1), and long-range (R=3). The method presented by Moore and Reynolds (1997) has been applied to determine the R ordering of the samples, by employing the *d*-spacing position of the 002/003 peak (which combines the Ilt 002 and EG smectite 003 reflections).

Thus the weight percentage of Ilt in the mixed-layer Ilt-Sme was evaluated by measuring the angular difference (°Δ2θ) between the 2θ position of peaks 001/002 and 002/003 of the mixed-layer Ilt-Sme and comparing it with tabulated values (Moore and Reynolds, 1997) (Table 3).

Structural B content in clayey sediments

Sediments were processed using a 0.1 M $MgCl_2$ solution with a Milli-Q B-free water (Moore and Reynolds, 1997), stirred, allowed to settle overnight, and rinsed twice with B-free water to remove the interlayer B hosted in Ilt-Sme and Sme phases. Samples (sediment/water ratio of 1:100) were subsequently washed with a 1.82% mannitol solution (Williams and Hervig, 2002), ultrasonicated, and stirred gently for 30 min while maintaining the temperature below 40°C. Samples were then rinsed with B-free water. Precautions were taken to prevent any loss of the clay fraction by centrifuging the samples, allowing all suspended material to settle between steps. The entire process was repeated three times using plastic beakers and centrifuge tubes to avoid any B contamination from borosilicate glassware. The absence of clay loss was confirmed by grain-size distribution analyses performed before and after the process. In addition, XRD analyses permitted the exclusion of any clay assemblages in the dark-colored supernatant, hypothesized to be organic matter, which appeared in several samples throughout the washing treatment. After the procedures for removal of interlayer and adsorbed species, the remaining B in the sample was considered to be bound to the crystalline structure (i.e. the B atoms replacing Si and Al in tetrahedral groups). Structure-bound or 'structural' B, referred to hereafter as B_{fix}, was assessed via prompt gamma neutron activation analysis (Actlabs Laboratories, Canada). The K_2O content was determined by inductively coupled plasma-optical emission spectroscopy (ICP-OES) of the clay fraction (<2 μm) after the mannitol and Mg^{2+} treatment.

The availability of K-rich fluids, associated primarily with the dissolution of K-feldspar and detrital mica, has traditionally been considered a key factor influencing the reduction of KI in Ilt during illitization (Offler and Prendergast, 1985; Scotchman, 1987; Kübler, 1990; Dellisanti et al., 2008), and this is evaluated in the Results section below.

Structural B (B_{fix}) in Ilt was calculated proportionally using the percentage of Ilt present in the clayey fraction of the samples (B_{fix} illite = B_{fix} clay × illite fraction; Table 4) because B is thought to enter the lattice of the Ilt phase preferentially with respect to the other clay phases (Środoń, 2010); however, Köster et al. (2019) reported that B in solution substitutes into the tetrahedral sites of Ilt-Sme by forming new illitic layers, and potentially into pure authigenic smectites; a B range of 110–150 ppm was reported by Ishikawa and Nakamura (1993) for B in marine smectite. Accordingly, and given the lack of target experimental data, the total B content was assumed for the clay-mineral phases from their percentage abundances.

Results and Discussion

The grain-size distribution showed significant homogeneity (Fig. 6). For all samples the silt fraction prevailed (62–75%), followed by clay (17–24%) and sand (5–17%) (the International Soil Science Society (ISSS) classification was used here). The samples were classified within fields VI and XII according to the Pettijohn classification system (1975).

The results indicated that in all analyzed samples the Ilt content was inversely correlated to Ilt-Sme (Fig. 7), as observed for Northern Apennines mud samples (Battaglia and Pennisi, 2016).
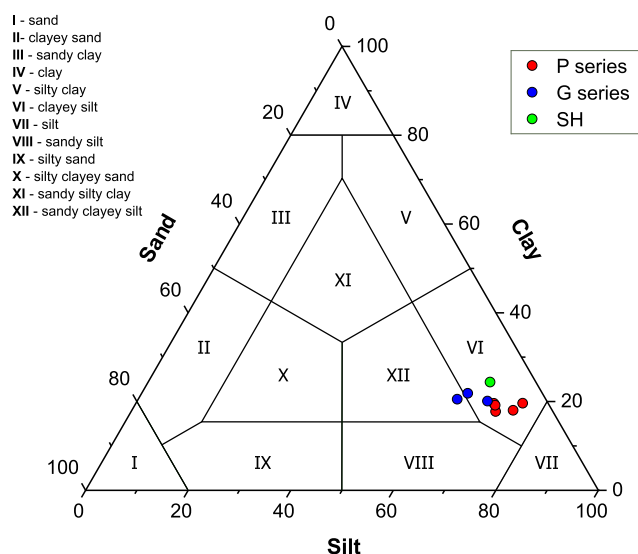
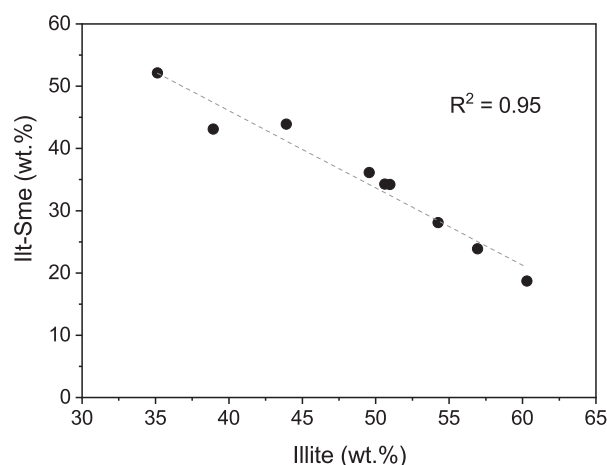**Figure 6.** Pettijohn classification diagram for the various sample sites.

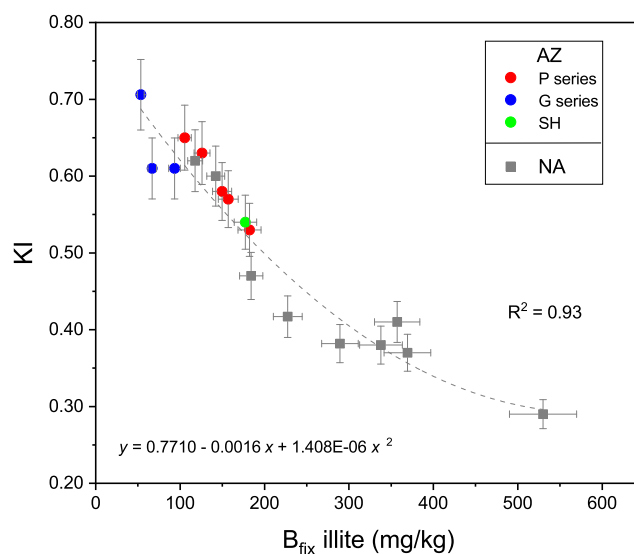**Figure 8.** Relationship between KI and structural B content in AZ and NA (NA data from Battaglia and Pennisi, 2016).

Figure 7. Inverse correlation between mixed-layer Ilt-Sme and illite.

Table 5. B content and isotope composition of waters from AZ mud volcanoes

ID	B (mg L^{-1})	δ^{11}B (‰)	SD (‰)
P1	99	50.8	0.16
P2	104	52.3	0.14
P3	92	47.9	0.07
P4	134	48.8	0.17
P5	88	53.6	0.11
G1	136	43.2	0.05
G2	151	39.7	0.16
G3	71	50.4	0.01
SH	144	43.2	0.11

This correlation suggested that for the samples studied, the mud source area had not reached the Ilt degradation zone (~4–6 km depth in the SCB; Buryakovsky et al., 1995). AZ mud samples showed a correlation between Ilt and mixed-layer Ilt-Sme, which was even greater than that observed in mud samples from NA. This is probably due to the smaller sampling area of the AZ campaign and, therefore, to a greater chemical-physical and mineralogical homogeneity. In AZ samples, the 'illite crystallinity' (expressed as KI) resulted in a positive correlation with structurally bound B in Ilt (Fig. 8). This may suggest that the samples belong to a common setting, with relatively small quantities of detrital Ilt compared with authigenic Ilt. The relation B$_{fix}$ – 'illite crystallinity' can be explained by the incorporation of B into the tetrahedral structure of Ilt that can increase crystallochemical homogeneity and reduce the structural defects such as atomic vacancies and lattice distortions (Moore and Reynolds, 1997). Despite the different geodynamic settings, KI *vs* B$_{fix}$ data from AZ and NA sites aligned with good approximation along the same trend, confirming and implementing the findings from Battaglia and Pennisi (2016). A narrower range of structural B values is again observed in the AZ samples with respect to NA samples (53 mg kg^{-1} < B$_{fix}$ illite < 182 mg kg^{-1}, and 118 mg kg^{-1} < B$_{fix}$ illite

< 530 mg kg^{-1}, respectively), which could also be related to the smaller sampling area investigated in AZ. The geochemical features observed could reasonably be related to the fluids associated with the extruded sediments. Relative to the seawater content (B = 5.0 mg L^{-1}; Gonfiantini et al., 2003), waters associated with erupted mud showed an enrichment in B of 3× to 16× in the NA samples and from 15× to 30× in the AZ samples (Table 5). The δ^{11}B signature ranged from +32‰ to +43‰ in NA samples (n. 6 data; M. Pennisi, unpublished data) and from +40‰ to +54‰ in AZ samples (n. 9 data; Salvadori, 2019) (Table 5). The chemical and isotopic signature of B may reflect different processes of B desorption *vs* B incorporation in the Ilt structure controlled by mud/water interaction occurring at different stages of diagenesis at the two sites (You et al., 1996; Kopf and Deyhle, 2002).

The Ilt (wt.%) *vs* B$_{fix}$ plot (Fig. 9) exhibits parallel regression lines, with that related to the AZ samples being shifted at higher Ilt values. Consequently, given a certain B$_{fix}$ concentration, AZ samples were systematically enriched in Ilt compared with NA, as a result.

William and Hervig (2002) proposed potassium concentration as a factor controlling KI. However, in the present study, as shown for the NA samples (Battaglia and Pennisi, 2016), a weak correlation between KI and K$_2$O content in sediments was observed (Fig. 10).
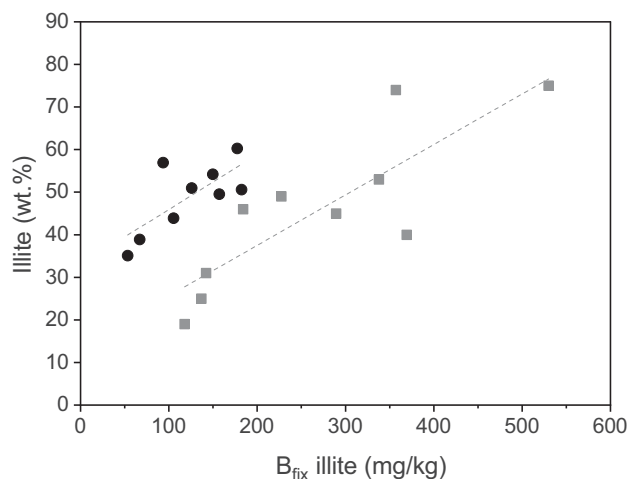
Figure 9. Positive correlation of Ilt content and B_{fix} for samples AZ (black circles) and NA (gray squares).
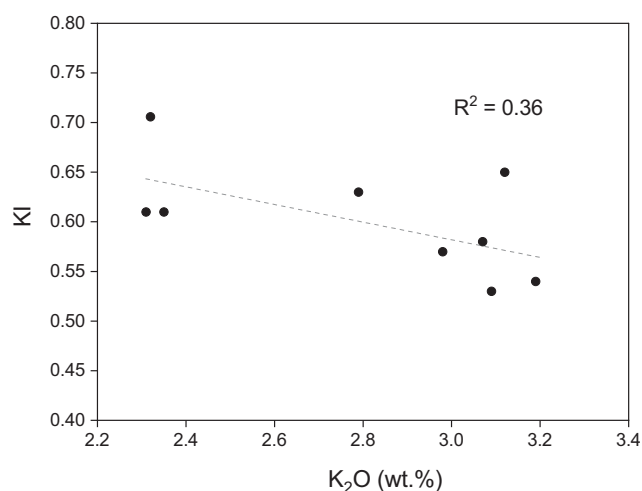

Figure 10. Weak correlation between KI and K content.

This study does not diminish or contradict the relationship between potassium and crystallinity, and no significant differences exist between the current study and previous research regarding the impact of K on 'illite crystallinity'. Therefore, in both contexts, the variation of KI appeared to be influenced mainly by temperature and B_{fix}.

To find an explanation for this and for the greater slope of the AZ regression in the plot of KI *vs* B_{fix} with respect to NA samples, we note that in NA mud volcanoes the temperature range supports the development of cyclic compounds at a depth of 5–6 km, given an average geothermal gradient of 25°C km^{-1} (Tassi et al., 2012), while in AZ this depth can be extended to 7–8 km, with an average geothermal gradient of 18°C km^{-1}. Furthermore, the gases emitted from AZ mud volcanoes are depleted in C$_{5+}$ alkanes relative to those from NA mud volcanoes, indicating that the AZ samples have undergone more extensive secondary processes (Bonini et al., 2013). This finding agrees with the deeper source estimated for the AZ mud volcanoes, identified in the Maykop formation (Hudson et al., 2008), and is also confirmed by the R1 Reichweite order of most samples that reflect a temperature range above 120°C (Merriman and Frey, 2009).

These results are consistent with previous conclusions about the maturity of hydrocarbon gases from SCB mud volcanoes, based on carbon isotopic composition and catagenetic maturity (Faber, 1987; Guliyev et al., 2001; Guliyev et al., 2004). Based on the vitrinite reflectance measurements in the SCB, it is likely that the ethane in the mud volcanoes examined was produced at depths of 7–8 km.

Conclusions

The present study provides significant insights into the impact of B content on the crystal structure of Ilt during the illitization of smectite and Ilt-Sme phases. This process influences the 'illite crystallinity' as quantified by Kübler's index. Observations were made in natural sedimentary basins characterized by the deposition of fine-grained sediments and the presence of B-enriched saline waters associated with mud volcanism, in Azerbaijan. The results agreed with the findings from a previous study on mud volcanoes in Italy, highlighting the correlation between structural B and KI across different geodynamic contexts and depositional environments. The AZ mud samples have shown a clayey silt composition, with the clay fraction ranging between 17 and 24%. The clay fraction consisted of smectite, illite, and mixed-layered minerals, indicating ongoing illitization, with Ilt content in the range of 35.1–60.3 wt.%. Boron-rich waters have been identified in association with mud extrusion. The comparison of the results obtained from the determination of the 'Reichweite' ordering parameter showed in AZ samples a greater degree of diagenesis (R1 order) compared with those from the NA (R1 for only 20% of the samples examined).

Physical, chemical, and mineralogical investigation of AZ mud samples allowed the authors to come to the following conclusions.

Investigation of Ilt in the mud volcanoes of Azerbaijan confirmed that the amount of structurally fixed B alters 'illite crystallinity' significantly.

Ilt crystallinity, expressed by the Kübler index (KI), and structurally fixed B (B_{fix}) were correlated by the equation KI = 0.771–0.00164 (B_{fix} illite) + $1.41 \cdot 10^{-6}$(B_{fix} illite)^2 (R^2=0.93) in mud from Azerbaijan (this work) and Northern Apennines of Italy. Note that this equation resulted from independent chemical and mineralogical data on samples from the two natural systems investigated, and not from experimental laboratory tests.

The correlation between B_{fix} in illite and the KI confirmed the finding that in young sedimentary basins where interaction occurs between clays and high-salinity B-rich waters, the application of the sediment-depth estimation method based on the determination of the KI on Ilt can be misleading. The correlation between KI and B in Ilt is, however, independent of the Ilt content. The present study, based on the study of a natural system in the context of sedimentary volcanism, aimed to address the key question of B_{fix}–'illite crystallinity' index relationship using a mineralogical and geochemical perspective. The present results could lay the groundwork for a more specific, in-depth crystallographic analysis of B incorporation in the Ilt structure.

References

Allen, M.B., Vincent, S.J., Alsop, G.I., Ismail-zadeh, A., & Flecker, R. (2003). Late Cenozoic deformation in the South Caspian region: effects of a rigid basement block within a collision zone. *Tectonophysics*, 366, 223–239.

Bailey, J.C. (2006). Geochemistry of boron in the Ilímaussaq alkaline complex, South Greenland. *Lithos*, 91, 319–330.

Baloglanov, E.E., Abbasov, O.R., & Akhundov, R.V. (2018). Mud volcanoes of the world: classifications, activities and environmental hazard (informational-analytical review). *European Journal of Natural History*, 5, 12–26.

Battaglia, S., Leoni, L., & Sartori, F. (2004). The Kübler index in late diagenetic to low-grade metamorphic pelites: a critical comparison of data from 10 Å and 5 Å peaks. *Clays and Clay Minerals*, 52, 85–105.

Battaglia, S., & Pennisi, M. (2016). Structural boron as factor controlling illite crystallinity in a mud volcano environment (Northern Apennine, Italy), *Chemical Geology*, 444, 120–127.

Berger, G., Velde, B., & Aigouy, T. (1999). Potassium sources and illitization in Texas Gulf Coast shale diagenesis. *Journal of Sedimentary Research*, 69, 151–157.

Bonini, M. (2012). Mud volcanoes: indicators of stress orientation and tectonic controls. *Earth-Science Reviews*, 115, 121–152.

Bonini, M., Tassi, F., Feyzullayev, A.A., Aliyev, C.S., Capecchiacci, F., & Minissale, A. (2013). Deep gases discharged from mud volcanoes of Azerbaijan: new geochemical evidence. *Marine Petroleum Geology*, 43, 450–463.

Brown, K.M. (1990). The nature and hydrogeologic significance of mud diapirs and diatremes for accretionary systems. *Journal of Geophysical Research Solid Earth*, 95, 8969–8982.

Buryakovsky, L.A., Djevanshir, R.D., & Chilingar, G. V. (1995). Abnormally-high formation pressures in Azerbaijan and the South Caspian Basin (as related to smectite↔illite transformations during diagenesis and catagenesis). *Journal of Petroleum Science and Engineering*, 13, 203–218.

Cavalcante, F., & Belviso, C. (2005). Trattamenti e metodi di preparazione di campioni di materiali argillosi per l'analisi diffrattometrica. Analisi Di Minerali Argillosi per Diffrazione Di Raggi X e Microscopia Elettronica. Teoria Ed ApplIcazioni. *Argille e minerali delle argille*, 5, 23–50 (in Italian).

Clauer, N., Williams, L.B., Lemarchand, D., Florian, P., & Honty, M. (2018). Illitization decrypted by B and Li isotope geochemistry of nanometer-sized illite crystals from bentonite beds, East Slovak Basin. *Chemical Geology*, 477, 177–194.

Colten-Bradley, V.A. (1987). Role of pressure in smectite dehydration – effects on geopressure and smectite-to-illite transformation. *American Association of Petroleum Geologists Bulletin*, 71, 1414–1427.

Couch, E.L., & Grim R.E. (1968). Boron fixation by illites. *Clays and Clay Minerals*, 16, 249–256.

Dellisanti, F., Pini, G., Tateo, F., & Baudin, F. (2008). The role of tectonic shear strain on theillitization mechanism of mixed-layers illite-smectite. A case study from a faultzone in the Northern Apennines, Italy. *Int. J. Earth Sci. 97*, 601–616.

Faber, E.Z. (1987). Isotopengeochemie gasformiger Kohlenwasserstoffe. *Erdole, Erdgas and Kohle*, 103, 210–218 (in German).

Fleet, M.E.L. (1965). Preliminary investigations into the sorption of boron by clay minerals. *Clay Minerals*, 6, 3–16.

Frederickson, A. F., & Reynolds, R. C. (1960). *Geochemical method for determining paleosalinity in clays and clay minerals* (ed. A. Swineford), pp. 203–213. Pergamon Press, The Netherlands.

Goldberg, E.D., & Arrhenius, G.O.S. (1958). Chemistry of Pacific pelagic sediments. *Geochimica et Cosmochimica Acta*, 13, 153–212.

Gonfiantini, R., Tonarini, S., Gröning, M., Adorni-Braccesi, A., Al-Ammar, M., Astner, A.S., Bächler, S., Barnes, R.M., Bassett, R.L., Cocherie, A., Deyhle, A., Dini, A., Ferrara, G., Gaillardet, J., Grimm, J., Guerrot, C., Krähenbühl, U., Layne, G., Lemarchand, D., Meixner, A., Northington, D.J., Pennisi, M., Reitznerová, E., Rodushkin, I., Sugiura, N., Surberg, R., Tonn, S., Wiedenbeck, M., Wunderli, S., Xiao, Y., & Zack T. (2003). Intercomparison of boron isotope and concentration measurements. Part II: Evaluation of results. *Geostandards Newsletter*, 27.

Guliyev, I.S., Feyzullayev, A.A., & Huseynov D.A. (2001). Isotope geochemistry of oils from fields and mud volcanoes in the South Caspian Basin, Azerbaijan. *Petroleum Geoscience*, 7, 409–417.

Guliyev, I.S., Huseynov, D.A., & Feyzullayev, A.A. (2004). Fluids of mud volcanoes in the Southern Caspian sedimentary basin: geochemistry and sources in light of new data on the carbon, hydrogen, and oxygen isotopic compositions. *Journal of Geochemistry International*, 42, 688–695.

Hillier, S., Matyas, J., Matter, A., & Vasseur, G. (1995). Illite/smectite diagenesis and its variable correlation with vitrinite reflectance in the Pannonian Basin. *Clays and Clay Minerals*, 43, 174–183.

Hudson, S.M., Johnson, C.L., Efendiyeva, M.A., Rowe, H.D., Feyzullayev, A.A., & Aliyev, C.S. (2008). Stratigraphy and geochemical characterization of the Oligocene-Miocene Maikop series: implications for the paleogeography of Eastern Azerbaijan. *Tectonophysics*, 451, 40–55.

Ishikawa, T., & Nakamura, E. (1993). Boron isotope systematics of marine sediments. *Earth and Planetary Science Letters*, 117, 567–580.

Keren, R. & O'Connor, G. A. (1982). Effect of exchangeable ions and ionic strength on boron adsorption by montmorillonite and illite. *Clays and Clay Minerals*, 30, 341–346.

Kopf A., & Deyhle A. (2002). Back to the roots: boron geochemistry of mud volcanoes and its implications for mobilization depth and global B cycling. *Chemical Geology*, 192, 195–210.

Kopf A., Deyhle A., Lavrushin, V.Y., Polyak, B.G., Gieskes, J.M., Buachidze, G.I., Wallmann, K., & Eisenhauer, A. (2003). Isotopic evidence (He, B, C) for deep fluid and mud mobilization from mud volcanoes in the Caucasus continental collision zone. *International Journal of Earth Science*, 92, 407–425.

Kopf, A.J. (2003). Global methane emission through mud volcanoes and its past and present impact on the Earth's climate. *International Journal of Earth Science*, 92, 806–816.

Köster, M.H., Williams, L.B., Kudejova, P., & Gilg, H.A. (2019). The boron isotope geochemistry of smectites from sodium, magnesium and calcium bentonite deposits. *Chemical Geology*, 510, 166–187.

Kübler, B. (1964). Les argiles, indicateurs de métamorphisme. *Revue de l'Institut Française du Pétrole*, 19, 1093–1112.

Kübler, B. (1967). La cristallinite de l'illite et les zones tout a fait superieures de metamorphisme. In *Etages Tectoniques*. Colloq. Neuchâtel 1966, A la Baconniere, 105–121.

Kübler, B. (1984). Les indicateurs des transformations physiques et chimiques dans la diagenese temperature et calorimetrie. *Thermométrie et Barométrie Géologiques*, 2, 489–596.

Kübler, B. (1990). Cristallinité de l'illite et mixed-layer: Bréve révision. *Schweiz. Mineral.Petrogr. Mitt. 70*, 89–93.

Lanson, B., Velde, B., & Meunier, A. (1998). Late-stage diagenesis of illitic clay minerals as seen by decomposition of X-ray diffraction patterns: contrasted behaviors of sedimentary basins with different burial histories. *Clays and Clay Minerals*, 46, 69–78.

Leoni, L. (2001). New standardized illite crystallinity data from low-to very-low grade metamorphic rocks (Northern Apennines, Italy). *European Journal of Mineralogy*, 13, 109–1118.

Lezzerini, M., Sartori, F., & Tamponi, M. (1995). Effect of amount of material used on sedimentation slides in the control of illite 'crystallinity' measurements. *European Journal of Mineralogy*, 7, 819–824.

Martos-Villa, R., Mata, M. P., Williams, L. B., Nieto, F., Arroyo, Rey X., & Sainz-Díaz, C. I. (2020). Evidence of hydrocarbon-rich fluid interaction with clays: clay mineralogy and boron isotope data from Gulf of Cádiz mud volcano sediments. *Minerals*, 10, 651.

Mazzini, A., & Etiope, G. (2017). Mud volcanism: an updated review. *Earth-Science Reviews*, 168, 81–112.

Merriman, R.J. & Frey, M. (2009). Patterns of very low-grade metamorphism in metapelitic rocks. In *Low-Grade Metamorphism* (ed. M. Frey and D. Robinson). Wiley: New Jersey.

Moore, D.M., & Reynolds, R.C. (1997). *X-ray Diffraction and the Identification and Analysis of Clay Minerals*. Oxford University Press, Oxford-New York, p. 378.

Murray, H. (2006). Structure and composition of the clay minerals and their physical and chemical properties. *Developments in Clay Science*, *2*, 7–31.

Nikitenko, O.A. & Ershov, V. V. (2021). Geochemical patterns of mud volcanic waters: reviewed worldwide data. *Geochemistry International*, *59*, 922–937.

Offler, R. & Prendergast, E. (1985). *Significance of illite crystallinity and bo values of K-white mica in low grade metamorphic rocks*, North Hill End Synclinorium, New South Wales Mineral. Mag.

Palmer, M.R., Spivack, A.J., & Edmond, J.M. (1987). Temperature and pH controls over isotopic fractionation during adsorption of boron on marine clay. *Geochimica et Cosmochimica Acta*, *51*, 2319–2323.

Pollastro, R.M. (1993). Considerations and applications of the illite/smectite geothermometer in hydrocarbon-bearing rocks of Miocene to Mississippian age. *Clays and Clay Minerals*, *41*, 119–133.

Reynolds, Jr, R.C. & Hower, J. (1970). The nature of interlayering in mixed-layer illite-montmorillonite. *Clays and Clay Minerals*, *18*, 25–36.

Reynolds, Jr, R.C. (1980). Interstratified clay minerals. In *Crystal Structures of Clay Minerals and their X-ray Identification* (ed. G. Brindley and G. Brown). Monograph 5, Mineralogical Society of Great Britain and Ireland, London.

Salvadori, M. (2019). *Sedimentary volcanism in Azerbaijan: a study on the origin of sediments emitted by the Perikushkul, Dashgil, and Shikhzahirli mud volcanoes and the effect of boron on controlling illite crystallinity*. University of Pisa (Master's thesis, in Italian).

Scotchman, I.C. (1987). Clay diagenesis in Kimmeridgian clay formation: onshore UK andits relation to organic maturation. *Mineral. Mag. 51*, 535–551.

Shannon, R. D. (1976). Revised effective ionic radii and systematic studies of interatomic distances in halides and chalcogenides. *Acta Crystallographica Section A*, *32*, 751–767.

Środoń, J. (2010). Evolution of boron and nitrogen content during illitization of bentonites. *Clays and Clay Minerals*, *58*, 743–756.

Stubican, V. & Roy, R. (1962). Boron substitution in synthetic micas and clays. *American Mineralogist*, *47*, 1166–1173.

Tassi, F., Fiebig, J., Vaselli, O., & Nocentini, M. (2012). Origins of methane discharging from volcanic-hydrothermal, geothermal and cold emissions in Italy. Chemical Geology, *310–311*, 36–48.

Varajao, A. & Meunier, A. (1996). Burial and thermal conditions of diagenesis in the Lower Cretaceous Barra de Itiuba Shale Formation, Sergipe-Alagoas basin, Brazil. (Enfouissement et conditions thermiques lors de la diagenese des shales de la formation de Barra de Itiuba, Cretace inferieure). *Bulletin de la Société Géologique de France*, *167*, 597–607.

Velde, B., Suzuki, T., & Nicot, E. (1986). Pressure-temperature-composition of illite/smectite mixed-layer minerals: Niger delta mudstones and other examples. *Clays and Clay Minerals*, *34*, 435–441.

Velde, B., & Vasseur, G. (1992). Estimation of the diagenetic smectite to illite transformation in time-temperature space. *American Mineralogist*, *77*, 967–976.

Warr, L. (2021) IMA-CNMNC approved mineral symbols. *Mineralogical Magazine*, *85*, 291–320.

Williams, L.B., & Hervig, R.L. (2002). Exploring intra-crystalline B-isotope variations in mixed-layer illite-smectite. *American Mineralogist*, *87*, 1564–1570.

Williams, L.B., Hervig, R.L., Holloway, J.R., & Hutcheon, I. (2001a). Boron isotope geochemistry during diagenesis. Part I. Experimental determination of fractionation during illitization of smectite. *Geochimica et Cosmochimica Acta*, *65*, 1769–1782.

Williams, L.B., Hervig, R.L., & Hutcheon, I. (2001b). Boron isotope geochemistry during diagenesis. Part II. Applications to organic-rich sediments. *Geochimica et Cosmochimica Acta*, *65*, 1783–1794.

Williams, L.B., Turner, A. & Hervig, R.L. (2007). Intracrystalline boron isotope partitioning in illite-smectite: testing the geothermometer. *American Mineralogist*, *92*, 1958–1965.

You, C.F., Spivack, A.J., Gieskes, J.M., Martin, J.B., & Davisson, M.L. (1996). Boron contents and isotopic compositions in pore waters: a new approach to determine temperature induced artifacts – geochemical implications. *Marine Geology*, *129*, 351–361.